

## Article

# Tempo-Spatial Variations in Soil Hydraulic Properties under Long-Term Organic Farming

M. Abu-hashim <sup>1,\*</sup> , H. Lilienthal <sup>2</sup>, E. Schnug <sup>2</sup>, Dmitry E. Kucher <sup>3</sup>  and Elsayed Said Mohamed <sup>3,4,\*</sup> <sup>1</sup> Soil Science Department, Faculty of Agriculture, Zagazig University, Zagazig 44519, Egypt<sup>2</sup> Julius Kühn-Institut—Federal Research Centre for Cultivated Plants, Institute for Crop and Soil Science, 38116 Braunschweig, Germany<sup>3</sup> Department of Environmental Management, Institute of Environmental Engineering, People's Friendship University of Russia (RUDN University), 6 Miklukho-Maklaya Street, 117198 Moscow, Russia<sup>4</sup> National Authority for Remote Sensing and Space Sciences, Cairo 11843, Egypt

\* Correspondence: dr.mabuhashim@gmail.com (M.A.); salama55@mail.ru (E.S.M.)

**Abstract:** Adequate knowledge of tempo-spatial variability on soil hydraulic properties plays an important role in irrigation scheduling and precision farming. This study was conducted to compare the impact of tempo-spatial variations in long-term conservation tillage applications in organic farming (superficial tillage using a chisel at 10 cm depth) on soil properties. Soil measurements, including infiltration capacity, saturated hydraulic conductivity (Ks), effective bulk density, and penetration resistance, were investigated in 2012 and compared to data from 2008 at the same fields in Baden-Württemberg, Germany. Long-term organic farming reflected a relative increase in Ks values with temporal variability 33% more in 2012 than in 2008, while soil texture was virtually time-invariant. The Ks increased from 27.06, 24.42, 40.46, 17.49, and 22.59 cm d<sup>-1</sup> in 2008 to 33.17, 28.79, 47.75, 38.99, and 40.82 cm d<sup>-1</sup> in 2012 for sample locations I, II, III, IV, and V, respectively. The effective bulk density values decreased from 1.72, 1.72, 1.68, 1.64, and 1.81 Mg m<sup>-3</sup> in 2008 to 1.63, 1.56, 1.67, 1.32, and 1.48 Mg m<sup>-3</sup> in 2012 for sample locations I, II, III, IV, and V, respectively. For spatial variations within the same season, variances in computed Ks values were attributed to differences in the soil textures and effective bulk density between different parcels. As the soil was managed by organic farming for a long time, the soil depth compactness was more pronounced in 2012 than in 2008. Nevertheless, the Ks values showed a temporal increase from 2008 to 2012 due to the preferential water flow pathways approach used in organic farming. Estimated Ks values by the Hydrus-1D model in 2012 were five times higher than in 2008. With soil depth, Ks values revealed a decreasing trend over time. Using the numerical model, Hydrus-1D was representative for comparing hydraulic parameters and simulating water transfer in the soil matrix.

**Keywords:** tempo-spatial variations; organic farming; infiltration capacity; hydraulic conductivity; soil compactness



**Citation:** Abu-hashim, M.; Lilienthal, H.; Schnug, E.; Kucher, D.E.; Mohamed, E.S. Tempo-Spatial Variations in Soil Hydraulic Properties under Long-Term Organic Farming. *Land* **2022**, *11*, 1655.

<https://doi.org/10.3390/land11101655>

Academic Editors: Rachid Mrabet, Haddioui Abdelmajid, Hamdali Hanane and Abbas Younes

Received: 31 July 2022

Accepted: 21 September 2022

Published: 25 September 2022

**Publisher's Note:** MDPI stays neutral with regard to jurisdictional claims in published maps and institutional affiliations.



**Copyright:** © 2022 by the authors. Licensee MDPI, Basel, Switzerland. This article is an open access article distributed under the terms and conditions of the Creative Commons Attribution (CC BY) license (<https://creativecommons.org/licenses/by/4.0/>).

## 1. Introduction

Tempo-spatial variations are naturally consistent with geologic and pedological influences on soil formation and changes in soil physical properties. For cropland, soil physical properties changes may occur due to differences in irrigation, tillage, and harvest/residue management [1–3]. Conventional and organic soil management are fundamentally different [4,5]. Conventional management (CM) implies monoculture cultivations with effects on soil structure that are mainly influenced by agricultural machinery, application of chemical fertilizers and pesticides, and crop roots. Otherwise, organic management (OM) is often a more complex approach whereby soil structure is affected by crop roots and other attributes, application of manures, intensive cultivations, and crop residues. These changes can be noticed from year to year and during cropping season according to climatic changes [4–6]. The volumetric water content and soil water retention have shown that even with tempo-spatial

changes over time for these properties, in contrast to soil hydraulic properties, their spatial structure did not change over time [7–10]. This phenomenon identifies a temporal/rank stability in spatial soil moisture [7] which is attributed to soil structure and topography. Although this stability has been studied for soil matric potential values, tempo-spatial variations in other hydraulic properties, such as the soil saturated hydraulic conductivity ( $K_s$ ), were not adequately investigated. In agricultural lands, Jarvis et al. [11] reported that tillage systems are considered an essential factor for temporal and spatial variations in the soil's physical characteristics. Hence, Strudley et al. [5] mentioned that for explaining spatial and temporal influences on  $K_s$ , field data collection should be enhanced in order to implement seasonal/annual measurement campaigns and elucidate short-term reactions. Soil hydraulic properties, mainly soil water retention and  $K_s$ , as parameters of water pressure head  $h$ , could be parameterized with analytical and numerical models [12,13]. Therefore, modeling the water flow increases the requirement for accurate measurements to compute the hydraulic characteristics [14,15]. Using analytical solutions, which reveal better assessment of different soil parameters, requires less computation and interference in soil water flow processes [14,16]. Nevertheless, van Genuchten and Nielsen [17] revealed that field and laboratory methods for determining soil hydraulic characteristics are costly and/or time-consuming. Laboratory methods are mainly based on Darcy's law [18] and the water-transient procedures involved in approximations of the Richards equation [14]. In contrast, more realistic results are built on field measurements than laboratory methods that keep the soil continuity versus depth [19]. Although field measurements are difficult to control, they are more representative of soil hydraulic properties. Therefore in situ measurements could more adequately estimate  $K_s$  compared to laboratory measurements [20]. Using the in situ field technique Hood infiltrometry/tension infiltrometry to investigate the soil hydraulic properties has gained increasing attention [21,22], particularly for estimating preferential water flow pathways. The advantage of this technique compared to others is that infiltration data and soil hydraulic properties are measured in situ [20]. Furthermore, this technique reduces soil disturbance and performs an investigation of the soil hydraulic characteristics of soil structure changes [23], tillage practices and land use changes [24], and plant roots [25]. Thus, the tension infiltrometer is suitable for estimating the tempo-spatial variation in soil hydraulic properties, as saturated soil hydraulic conductivity is a key parameter for studying and modeling water fluxes and contaminant transport within the vadose zone. The objectives of this study were: (i) to identify the impact of tempo-spatial variations on soil hydraulic characteristics in long-term organic farming, and (ii) to estimate water transfer within the soil using the Hydrus-1D numerical approach at plot scale.

## 2. Materials and Methods

### 2.1. Description of Study Area

Field measurements were conducted in 2008 and 2012 in Brehmen village (3537244, 5494266, Gauß Krüger, Zone 3) at the catchment area of the river Tauber, where the same organic farming procedures of no-tillage management (superficial tillage using a chisel at 10 cm depth) with turning over the residues of crops after harvest on the soil surface, have been applied in this region since 2001 (Figure 1).



**Figure 1.** Sample field location of Brehmen village, Tauberbischofsheim, southern Germany.

The test site is situated east of Tauberbischofsheim, in the northeastern district of Baden-Württemberg, Germany. Study areas are located 310–430 m above sea level. The average annual precipitation and temperature are 732 mm and 8.6 °C, respectively (DWD, 2012). The soil is Luvisols, mainly developed on limestone material. Crop rotation of the five fields under organic farming was investigated from 2008 to 2012 (Table 1).

**Table 1.** Crop rotation from 2008 to 2012 of the investigated fields.

Sample Location	Crop Type				
	2008	2009	2010	2011	2012
I	Spelt	Flax	Black emmer	Alfalfa	Alfalfa
II	Spelt	Sweet pea	Red clover	Red clover	Winter Wheat
III	Winter rape	Winter Wheat	Summer barley	Spelt	Barley
IV	Oats	Barley	Rye	Summer wheat	Black emmer
V	Winter Wheat	Red clover	Red clover	Winter Wheat	Spelt

## 2.2. Field Soil Measurements

The experimental field was homogeneous at each location in most respects (climate conditions, irrigation processes, agronomical practices, and crop types), and small variations among the investigated fields reflect the impact of temporal variations.

The infiltration rate of water through the soil surface was investigated using the Hood infiltrometer device [20]. This instrument allows measurement of the steady-state infiltration rate ( $q_s$ ). On the soil surface, the amount of water infiltrating each 30 s was monitored over time until reaching a steady infiltration state (Figure 2).

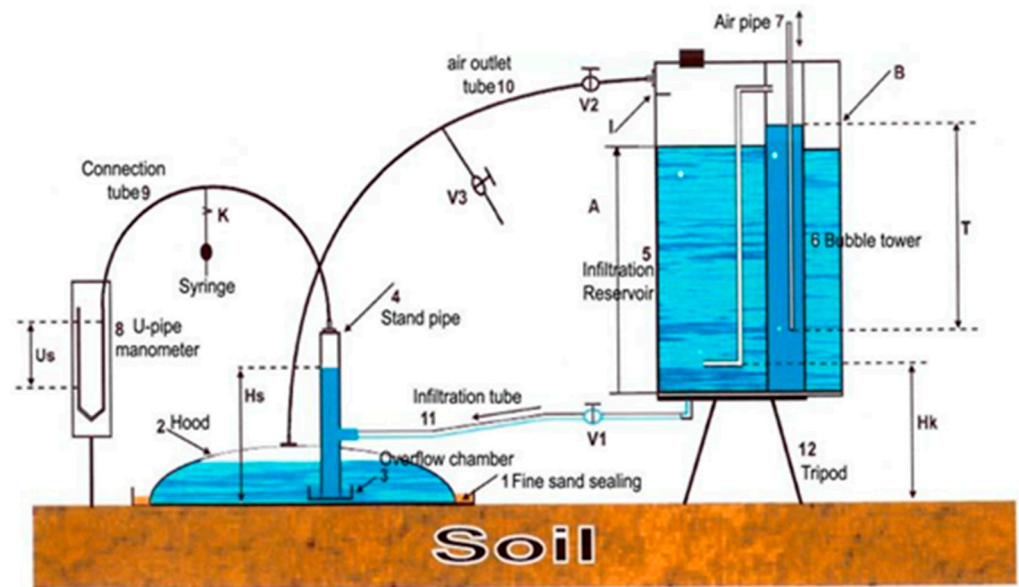


Figure 2. Principles of infiltration measurement using a Hood infiltrrometer [20].

During the process, the last five readings at the steady state were averaged, and the steady flow rate was recorded. Compared with the disc infiltrmeter, the Hood infiltrmeter did not require preparation of the soil surface, and no contact material and/or perforated plate was required on the infiltration soil surface (Figure 2). Thus, measurements using the Hood infiltrmeter reflect many physical properties of the soil surface, such as soil compaction and silting [20,22]. Soil dry bulk density ( $\rho_b$ ) at the investigated sites and the initial water content (near the hood location) were examined by collecting undisturbed soil samples from several soil depths, 0–10, 10–20, and 20–30 cm, using a standard metal soil core with a volume of 100 cm<sup>3</sup> [26], and three replicates at each soil horizon. For routine physical measurements (Table 2), composite soil samples were analyzed from the 0–10 cm soil layer that was close to the infiltration site [27].

Table 2. Physical properties of the investigated sample locations.

Sample Location	X_Coord	Y_Coord	Soil Management	Particle Size Distribution			Texture
				Sand%	Silt%	Clay%	
I	3540422	5492031	Organic	2.1	52.1	45.8	Clay
II	3541030	5491781	Organic	11.3	52.1	36.5	Silty Clay Loam
III	3539854	5491288	Organic	3.3	44.3	52	Clay
IV	3539806	5492396	Organic	3.3	63	33.7	Silty Clay Loam
V	3539646	5492708	Organic	1.2	60.9	37.8	Silty Clay Loam

For all the investigated sites, the steady-state infiltration rate was measured at a pressure head of  $-1$  cm, and sample measurements were taken as three replicates for each sample location in 2008 and 2012 at the same X, Y coordinates (Table 2). Data collected in the field were flow rates ( $Q_s$ ), which were converted into steady infiltration rates ( $q_s$ ) according to [28] in the following equation:

$$q_s = \frac{Q_s}{\pi \cdot r^2} \tag{1}$$

where  $Q_s$  is the steady flow rate [L<sup>3</sup> L<sup>-1</sup>],  $r$  is the radius of the hood (L), and  $q_s$  is the steady-state infiltration rate [L.T<sup>-1</sup>]. Infiltration data using the Hood infiltrmeter were based mainly on Wooding’s analytical method [20]. Thus, with the determination of  $Q_s$ ,

the unsaturated hydraulic conductivity of the investigated soil was computed according to [29]:

$$q_s = K_u \cdot \left( 1 + \frac{4}{\pi \cdot r \cdot \alpha} \right) \quad (2)$$

where  $K_u$  is the unsaturated soil hydraulic conductivity [L.T-1] and  $\alpha$  is the sorptivity number of the soil [L-1]. The soil sorptivity number ( $\alpha$ ) is a constant equal to the reference value of  $0.12 \text{ cm}^{-1}$  for agriculture soils [30]. Computing the unsaturated hydraulic conductivity using Wooding's equation, the saturated hydraulic conductivity ( $K_s$ ) was calculated according to Gardner's equation [12]:

$$K_s = \frac{K_u}{\exp(\alpha \cdot h)} \quad (3)$$

where  $K_s$  is the saturated hydraulic conductivity (L.T-1), and  $h$  is the pressure head (L).

### 2.3. Degree of Compactness Calculations

#### 2.3.1. Effective Bulk Density

Heavy clay soils are affected by swelling and shrinking processes. Thus, the soil dry bulk density ( $\rho_b$ ) is not considered a relevant tool for reflecting the degree of soil compactness. Kelishadi and Mosaddeghi [31] revealed that  $\rho_b$  may be high in soils with higher clay content but might not be crucial in coarse-textured soil at the same value. Bulk density generally cannot reflect the degree of soil compactness that results from plant root growth and crop yield [32].

This could be attributed to the dependence of BD on many factors other than texture, including soil organic matter content and clay mineralogy type. Therefore, the effective bulk density (eBD) considers these factors [22,31,33]. The eBD s computed according to the following equation [33]:

$$eBD \left( \text{Mg m}^{-3} \right) = \rho_b + 0.009 \cdot C_c \quad (4)$$

where  $\rho_b$  is the soil dry bulk density ( $\text{Mg m}^{-3}$ ), and  $C_c$  is the clay content ( $\text{kg.100 kg}^{-1}$ ).

#### 2.3.2. Penetration Resistance

Soil penetration resistance was investigated using a Penetrologger Eijkelkam UGT-Art.-Nr.: 5060407. The Penetrologger Eijkelkam consists mainly of an electronic penetrometer coupled with a data logger, which is implemented for storing and processing the measurement data and probing rods with different cones. For field measurements, the penetrologger was set to a depth of 50 cm.

At the investigated site, for each sample location in 2008 and 2012 at the same X, Y coordinates, the probing rod with a proper cone at the defined point was propelled into the soil. The soil resistance values to probing rod penetration at each soil layer of the ground profile were measured and saved in the data logger. The measurements were performed with 10 replicates at each investigation site and measurement point.

### 2.4. Simulation of One-Dimensional Water Flow

To simulate water transfer in the variably saturated soil in 2008 and 2012, the HYDRUS-1D model applied in the current work was numerically provided by the method of [34]. In addition, the HYDRUS-1D code primarily depended on the Richards equation for the one-dimensional water flow. The flow was explained by the equation:

$$\frac{\partial \theta(h, t)}{\partial t} = \frac{\partial}{\partial z} \left[ k(h) \left( \frac{\partial h}{\partial z} + 1 \right) \right] \quad (5)$$

where  $\theta$ : is volumetric water content,  $h$  is soil water pressure head,  $k(h)$  is unsaturated hydraulic conductivity,  $z$  is the vertical coordinate at the soil surface (negative down-

ward), and  $t$  is time. The initial condition and upper boundary condition for the studied experiment were:

$$h(0,t) = h_0 \quad (6)$$

$$h(z,0) = h_i(z) \quad (7)$$

where  $h_0$  is the water potential at the upper soil surface, and  $h_i(z)$  is the initial water pressure head within the soil column. The van Genuchten–Mualem model was utilized for the selected areas [35]. The HYDRUS-1D code is connected mainly with the ROSETTA model of [36]. For the boundary conditions in this investigation, we used the van Genuchten–Mualem model with non-hysteresis to study the soil hydraulic properties for all sites. The upper boundary conditions for the investigated sites were in pressure head  $-1$  cm, which was applied during the infiltration rate experiment using the Hood infiltrometer, while the lower boundary condition was free drainage.

### 3. Results and Discussions

#### 3.1. Infiltration Measurements

Analysis of the Hood infiltrometer dataset in situ helped our understanding of the soil hydraulic parameters and in comparing the field results at tempo-spatial variations. Table 3 shows the saturated hydraulic conductivity values obtained using the Gardner equation. Before explaining the results, it is worth acknowledging that the experimental fields at each location were homogeneous in most aspects, such as the irrigation regime, climate conditions, agronomical management, and crop types, such that small variations among investigated fields would reflect the differences of  $K_s$  in temporal variations under long-term organic farming since the soil texture is virtually time-invariant. At the field scale,  $K_s$  measurements showed a relative increase in their values from 2008 to 2012, excluding location Nr. 1 (Table 3). The average relative increases of  $K_s$  values in 2012 were 33% higher than their values in 2008. However, the variances in  $K_s$  values within the same season could be attributed to the differences in the soil textures and effective soil dry bulk density values among the different parcels (Table 2).

**Table 3.** Soil physical properties in 2008 and 2012 field campaigns under organic farming.

Year	Property	Field Location				
		I	II	III	IV	V
2008	BD ( $\text{Mg m}^{-3}$ )	1.31	1.39	1.21	1.34	1.47
	$e$ BD ( $\text{Mg m}^{-3}$ )	1.72	1.72	1.68	1.64	1.81
	$q_s$ ( $\text{cm min}^{-1}$ )	1.84	0.67	1.11	0.48	0.62
	$K_s$ ( $\text{cm d}^{-1}$ )	27.06	24.42	40.46	17.49	22.59
2012	BD ( $\text{Mg m}^{-3}$ )	1.22	1.23	1.20	1.02	1.14
	$e$ BD ( $\text{Mg m}^{-3}$ )	1.63	1.56	1.67	1.32	1.48
	$q_s$ ( $\text{cm min}^{-1}$ )	0.91	0.79	1.31	1.07	1.12
	$K_s$ ( $\text{cm d}^{-1}$ )	33.17	28.79	47.75	38.99	40.82

BD: bulk density;  $e$ BD: effective bulk density;  $q_s$ : steady-state flow infiltration rate;  $K_s$ : saturated hydraulic conductivity.

Results are in agreement with [37,38] that  $K_s$  considerably varied in space and time. However, Chirico et al. [39] revealed that the relationship between  $K_s$  and other soil parameters, such as bulk density and soil texture, is not adequate for the accurate prediction of  $K_s$  values. As soil texture is temporarily invariant, variation in  $K_s$  values could be explained by long-term organic farming. Consequently, we argue such changes in  $K_s$  values from 2008 to 2012 were due to the soil biopores effect. Poudel et al. [40] revealed that organic management led to a relevant soil structure and efficient infiltration capacity in soil [41]. Thus, organic farming has become an efficient procedure to reverse the consequences of anthropogenic sealing effects on soil [42].

The results in Table 3 show that eBD values decreased from 2008 to 2012, and this decreasing trend is consistent with increasing  $K_s$  values from 2008 to 2012. This trend might be due to the high frequency of soil micro-pore creation as a result of continuous organic farming [22,31,41]. In contrast to these results, soil penetration resistances obtained by the penetrometer device indicated another phenomenon. Soil penetration resistance values in the investigated soils were lower in 2008 than in 2012 (Figure 3).

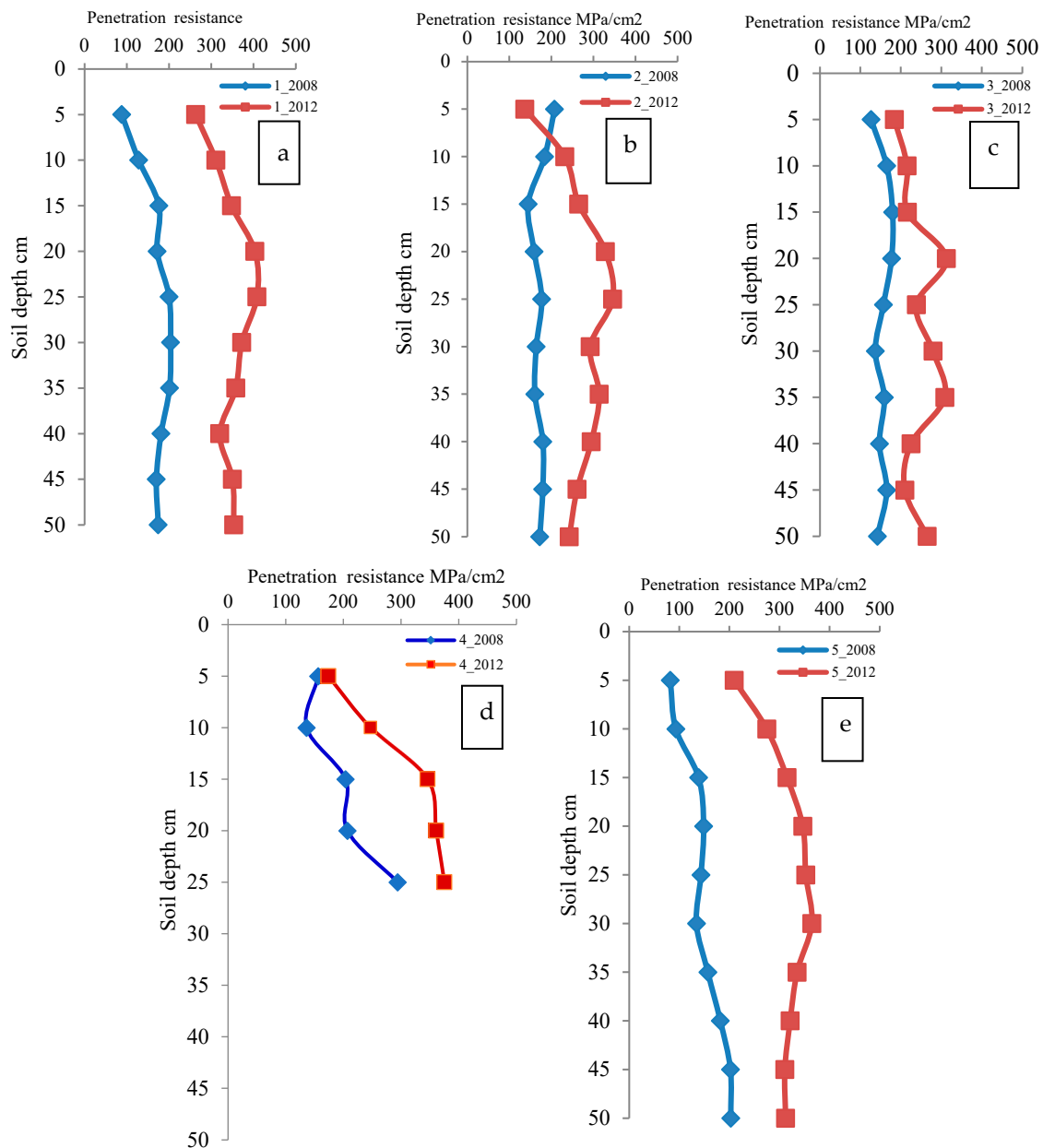


**Figure 3.** Penetration resistance with soil depth for field locations; (a–e) under organic farming in 2008 and 2012.

These results showed that even though the soil was managed by organic farming for a long time, compactness was more pronounced with deep soil in 2012 compared to 2008. This could be attributed to the macro-pores resulting from the absence of deep ploughing during organic farming processes and the presence of hardpans that did not allow the penetrometer probe to penetrate the soil deeper than 25 cm in location Nr. 4; thus, the measurements in location Nr. 4 were recorded only to a soil depth of 25 cm. Nevertheless,  $K_s$  results revealed a temporal increase from 2008 to 2012 (Table 3) that could be explained

by the preferential water flow pathways approach that reveals a greater number of biopores in the soil [40,41]. These results revealed that the tillage system in the field is the main factor that affects soil quality, irrespective of clay content [21,42].

### 3.2. Simulation of One-Dimensional Water Flow

Table 4 displays results for the hydrological parameters of soils under temporal variations from 2008 and 2012. Using one soil type (Silty Clay Loam) of sample location Nr. 4, the impact of temporal variation on soil hydrological parameters was investigated using the Hydrus-1D code. By implementing in situ measured saturated hydraulic conductivity analysis under different land management, particle size distribution, and bulk density in the Hydrus-1D model, the hydrological parameters ( $Q_r$ ,  $Q_s$ ,  $\alpha$ , and  $n$ ) were optimized (Table 4). The results revealed that  $K_s$  values estimated by the numerical Hydrus-1D method in 2012 were five times higher than in 2008.

**Table 4.** Hydraulic properties of sampled soils under organic farming in 2008 and 2012.

Field Management	Soil Type	Theta r ( $\text{cm}^3 \text{cm}^{-3}$ )	Theta s ( $\text{cm}^3 \text{cm}^{-3}$ )	Alpha (1/cm)	n	$K_s$ ( $\text{cm.h}^{-1}$ )
Org. (2008)	Silty Clay Loam	0.091	0.481	0.09	1.502	0.472
Org. (2012)	Silty Clay Loam	0.098	0.574	0.01	1.467	2.323

Theta r ( $Q_r$ ): residual water content ( $\text{cm}^3 \text{cm}^{-3}$ ); theta s ( $Q_s$ ): saturated water content ( $\text{cm}^3 \text{cm}^{-3}$ );  $K_s$ : saturated hydraulic conductivity ( $\text{cm d}^{-1}$ ); alpha: sorptivity number (1/cm); n: pore-size distribution index.

Most one-dimensional simulation models based on the Richards equation failed to clarify the possible occurrence of unstable water flow [17]. However, in field trials, the preferential flow may partly account for the inadequate prediction of water movement. We recommend that numerical models are adapted to in situ field measurements to account for the water flow phenomenon and to achieve maximum benefit. In addition, the numerical results show that modeling soil water flow would require precise measurements of the soil's physical properties to estimate the soil's hydraulic characteristics [43–46]. The obtained results were consistent with the field experiments of [14,47], which imposed the water pressure head through a tension infiltrometer. The results of Figure 4 show that the saturated hydraulic conductivity reveals a logarithmic decrease with the pressure head distribution in the soil matrix (0–30 cm) and that the impact of long-term cultivation under organic farming was predominant. The  $K_s$  values versus soil depth were identified using the Hydrus-1D model (Figure 4). Simulated  $K_s$  distributions at depth 5 cm were 0.213 and 0.264 cm/hour after half and one hour in 2008, while their value distributions were 1.371 and 1.867 cm/hour in 2012 for the same spatio-temporal variation with soil depth, respectively (Figure 5). With soil depth,  $K_s$  values revealed decreasing values over time. Nevertheless, this decreasing trend shows that the  $K_s$  distribution values obtained in 2012 were six times higher than in 2008 versus soil depth (5 cm) within the first two hours, while their distribution values in 2012 were nine times higher than in 2008 versus soil depth (10 cm) within the first two hours. This was interpreted due to an increasing wetting front, higher biological activity [40], more soil biopores [42], and higher infiltration capacity. In addition, the results indicate that  $K_s$  values approximately reached the steady state in both 2008 and 2012 after 6 h, which could be attributed to the steady-state flow rate becoming constant.

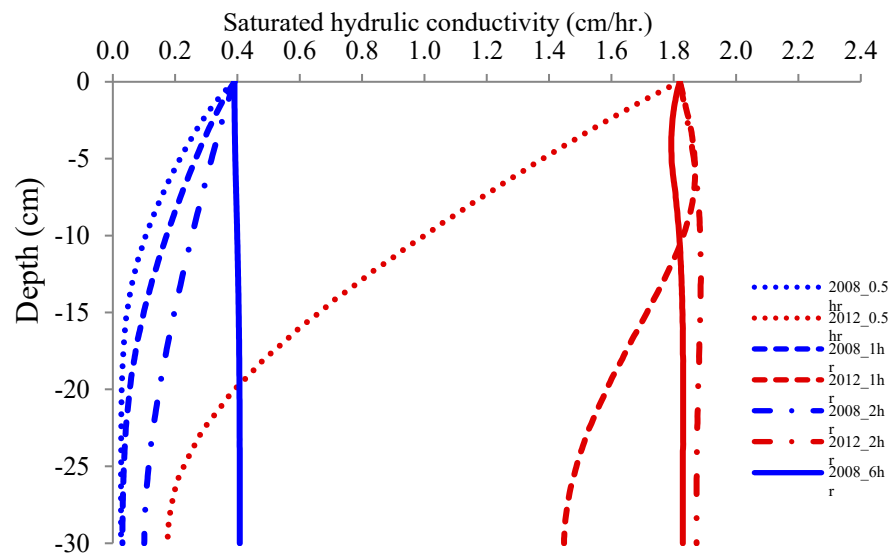


**Figure 4.** Saturated hydraulic conductivity changes with depth under organic management using the numerical Hydrus-1D model in 2008 and 2012.

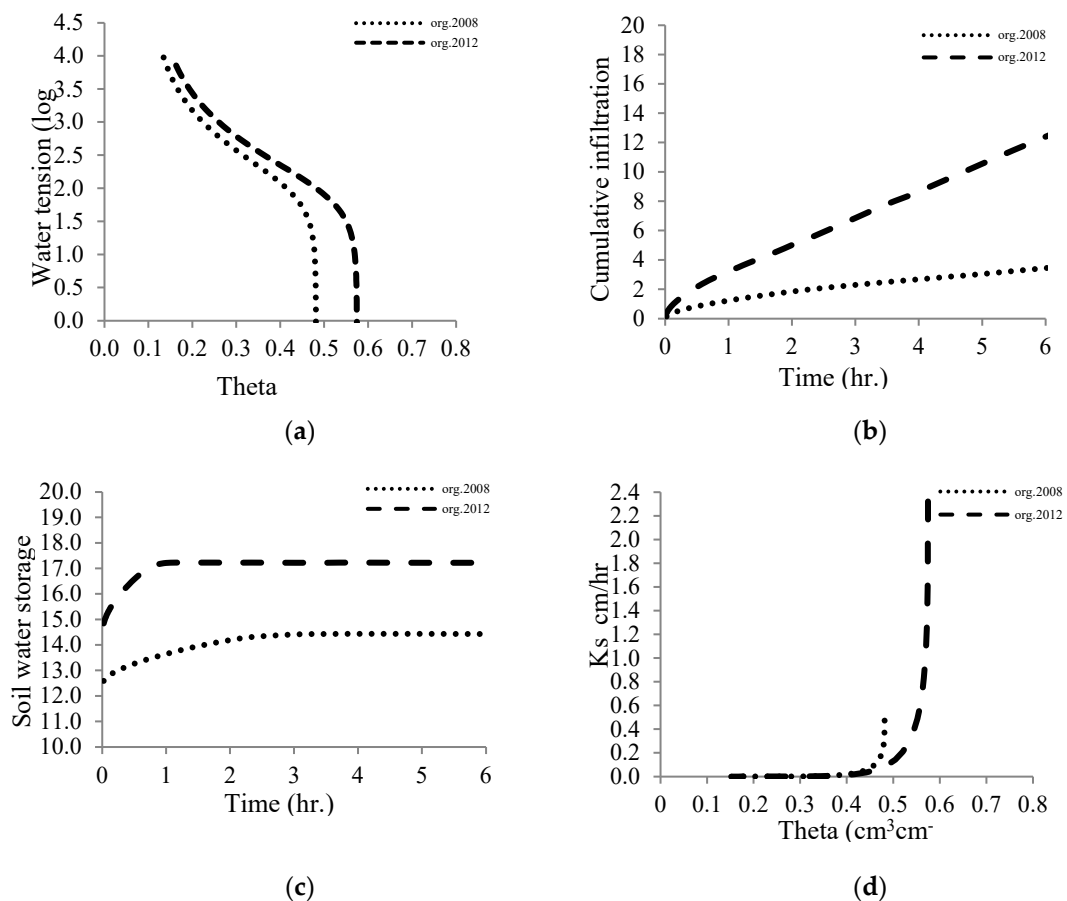


**Figure 5.** Hydraulic properties under organic management, (a) water retention curves, (b) cumulative infiltration versus time, (c) soil water storage capacity versus time, (d) saturated hydraulic conductivity versus volumetric water content.

Using the numerical Hydrus-1D model, the impact of temporal variation on soil water flow was estimated (Figure 5). Figure 5a shows the water retention curves under the impact of long-term cultivation with organic farming. Distinct differences were detected,

whereby the volumetric water content in 2012 revealed an increase in the field capacity compared to 2008. Volumetric water content at the field capacity was  $0.318 \text{ cm}^3 \text{ cm}^{-3}$  and  $0.367 \text{ cm}^3 \text{ cm}^{-3}$  in 2008 and 2012, respectively, and these differences were apparent with the decreasing trend in water tension. The cumulative infiltration curve under OM in 2012 was greater than in 2008 (Figure 5b), and this result was in agreement with the effects of water retention during the infiltration process. These results corresponded well with Ks versus the volumetric water content (Figure 5d), which reflected the same trend of increasing Ks under OM in 2012 compared to OM in 2008, with increasing the volumetric water content in soils. In addition, the soil required 3 h under OM to reach the constant storage capacity in 2008 compared to 2012, which required 1 h (Figure 5c). Our results are in agreement with [48,49] that organic farming is often considered a relevant farming system. Thus, long-term organic farming influences volumetric content on the soil surface and affects soil hydraulic parameters [24,50–53].

#### 4. Conclusions

Selecting tillage practices without ploughing maintains long-term soil quality and, subsequently, yields more interest in organic farming. Long-term organic farming revealed a relative increase in soil saturated hydraulic conductivity (Ks) values with temporal variations since soil texture is virtually time-invariant. However, variance in the computed Ks values within the same season was attributed to a difference in soil textures and effective bulk density values between different parcels. Even though the soil was managed by organic farming for a long time, more compactness was pronounced in the deep soil, which resulted from the absence of deep ploughing during organic farming processes. Nevertheless, long-term organic farming has become an efficient procedure to counteract the consequences of anthropogenic sealing of cropland by enhancing the preferential water flow pathways.

**Author Contributions:** Conceptualization: M.A.-h., E.S.M., E.S. and H.L.; introduction: M.A.-h., H.L. and E.S.M.; methodology: E.S. and E.S.M.; results and discussion: E.S. and E.S.M.; review and conclusions: E.S.M., M.A.-h. and D.E.K. All authors have read and agreed to the published version of the manuscript.

**Funding:** This research received no external funding.

**Data Availability Statement:** Not applicable.

**Acknowledgments:** The authors would like to acknowledge the Soil Department, Faculty of Agriculture, Zagazig University, the Institute for Crop and Soil Science, and the Julius Kühn-Institut, Braunschweig, Germany. This paper was supported by the RUDN University Strategic Academic Leadership Program.

**Conflicts of Interest:** The authors declare no conflict of interest.

#### References

1. Mubarak, I.; Mailhol, J.C.; Angulo-Jaramillo, R.; Ruelle, P.; Boivin, P.; Khaledian, M. Temporal variability in soil hydraulic properties under drip irrigation. *Geoderma* **2009**, *150*, 158–165. [[CrossRef](#)]
2. Vakali, C.; Zaller, J.G.; Köpke, U. Reduced tillage effects on soil properties and growth of cereals and associated weeds under organic farming. *Soil Tillage Res.* **2011**, *111*, 133–141. [[CrossRef](#)]
3. Abu-hashim, M.; Mohamed, E.; Belal, A. Land-use changes and site variables on the soil organic carbon pool: The potential application for the MENA region. *Adv. Environ. Res.* **2017**, *55*, 65–100.
4. Peigné, J.; Vian, J.-F.; Payet, V.; Saby, N.P. Soil fertility after 10 years of conservation tillage in organic farming. *Soil Tillage Res.* **2018**, *175*, 194–204. [[CrossRef](#)]
5. Strudley, M.W.; Green, T.R.; Ascough, J.C., II. Tillage effects on soil hydraulic properties in space and time: State of the science. *Soil Tillage Res.* **2008**, *99*, 4–48. [[CrossRef](#)]
6. Abu-hashim, M.; Elsayed, M.; Belal, A.-E. Effect of land-use changes and site variables on surface soil organic carbon pool at Mediterranean Region. *J. Afr. Earth Sci.* **2016**, *114*, 78–84. [[CrossRef](#)]
7. Vachaud, G.; Passerat de Silans, A.; Balabanis, P.; Vauclin, M. Temporal stability of spatially measured soil water probability density function. *Soil Sci. Soc. Am. J.* **1985**, *49*, 822–828. [[CrossRef](#)]

8. Chen, J.; Hopmans, J.W.; Fogg, G.E. Sampling design for soil moisture measurements in large field trials. *Soil Sci.* **1995**, *159*, 155–161. [[CrossRef](#)]
9. Abdel-Fattah, M.K.; Abd-Elmabod, S.K.; Aldosari, A.A.; Elrys, A.S.; Mohamed, E.S. Multivariate analysis for assessing irrigation water quality: A case study of the Bahr Mouise Canal, Eastern Nile Delta. *Water* **2020**, *12*, 2537. [[CrossRef](#)]
10. Mohamed, E.S.; Abu-hashim, M.; AbdelRahman, M.A.; Schütt, B.; Lasaponara, R. Evaluating the effects of human activity over the last decades on the soil organic carbon pool using satellite imagery and GIS techniques in the Nile Delta Area, Egypt. *Sustainability* **2019**, *11*, 2644. [[CrossRef](#)]
11. Jarvis, N.; Zavattaro, L.; Rajkai, K.; Reynolds, W.; Olsen, P.-A.; McGechan, M.; Mecke, M.; Mohanty, B.; Leeds-Harrison, P.; Jacques, D. Indirect estimation of near-saturated hydraulic conductivity from readily available soil information. *Geoderma* **2002**, *108*, 1–17. [[CrossRef](#)]
12. Gardner, W. Mathematics of isothermal water conduction in unsaturated soils. *Highw. Res. Board Spec. Rep.* **1958**, *40*, 78–87.
13. Genuchten, M.T.V. General approach for modeling solute transport in structured soils. *Report* **1985**, *19*, 513–526.
14. Šimůnek, J.; Angulo-Jaramillo, R.; Schaap, M.G.; Vandervaere, J.-P.; Van Genuchten, M.T. Using an inverse method to estimate the hydraulic properties of crusted soils from tension-disk infiltrometer data. *Geoderma* **1998**, *86*, 61–81. [[CrossRef](#)]
15. Haverkamp, R.; Debionne, S.; Angulo-Jaramillo, R.; de Condappa, D. Soil properties and moisture movement in the unsaturated zone. In *The Handbook of Groundwater Engineering*; CRC Press: Boca Raton, FL, USA, 2016; pp. 167–208.
16. Wöhling, T.; Vrugt, J.A. Combining multiobjective optimization and Bayesian model averaging to calibrate forecast ensembles of soil hydraulic models. *Water Resour. Res.* **2008**, *44*, W12432. [[CrossRef](#)]
17. Van Genuchten, M.T.; Nielsen, D. On describing and predicting the hydraulic properties. *Ann. Geophys.* **1985**, 615–628.
18. Corey, A.T. 3.6. 1.1 Laboratory. *Methods Soil Anal. Part 4 Phys. Methods* **2002**, *5*, 899–936.
19. Ramos, T.; Goncalves, M.; Martins, J.; Van Genuchten, M.T.; Pires, F. Estimation of soil hydraulic properties from numerical inversion of tension disk infiltrometer data. *Vadose Zone J.* **2006**, *5*, 684–696. [[CrossRef](#)]
20. Schwärzel, K.; Punzel, J. Hood infiltrometer—A new type of tension infiltrometer. *Soil Sci. Soc. Am. J.* **2007**, *71*, 1438–1447. [[CrossRef](#)]
21. Wahren, A.; Feger, K.-H.; Schwärzel, K.; Münch, A. Land-use effects on flood generation—considering soil hydraulic measurements in modelling. *Adv. Geosci.* **2009**, *21*, 99–107. [[CrossRef](#)]
22. Abu-Hashim, M.S.D. Impact of Land-Use and Land Management on Water Infiltration Capacity on a Catchment Scale, in Fakultät Architektur. Ph.D. Thesis, Bauingenieurwesen und Umweltwissenschaften der Technischen Universität Carolo-Wilhelmina zu Braunschweig, Braunschweig, Germany, 2011.
23. Hussen, A.; Warrick, A. Alternative analyses of hydraulic data from disc tension infiltrometers. *Water Resour. Res.* **1993**, *29*, 4103–4108. [[CrossRef](#)]
24. Bodhinayake, W.; Cheng Si, B. Near-saturated surface soil hydraulic properties under different land uses in the St Denis National Wildlife Area, Saskatchewan, Canada. *Hydrol. Process.* **2004**, *18*, 2835–2850. [[CrossRef](#)]
25. Clothier, B.; White, I. Measurement of sorptivity and soil water diffusivity in the field. *Soil Sci. Soc. Am. J.* **1981**, *45*, 241–245. [[CrossRef](#)]
26. Carter, M.R.; Gregorich, E.G. *Soil Sampling and Methods of Analysis*; CRC Press: Boca Raton, FL, USA, 2007.
27. Klute, A. Water retention: Laboratory methods. In *Methods of Soil Analysis. Part 1. Agronomy Monograph 9*; Klute, A., Ed.; ASA, SSSA: Madison, WI, USA, 1986; Volume 3, pp. 635–662.
28. Reynolds, W.; Elrick, D. Determination of hydraulic conductivity using a tension infiltrometer. *Soil Sci. Soc. Am. J.* **1991**, *55*, 633–639. [[CrossRef](#)]
29. Wooding, R. Steady infiltration from a shallow circular pond. *Water Resour. Res.* **1968**, *4*, 1259–1273. [[CrossRef](#)]
30. Rienzner, M.; Gandolfi, C. Investigation of spatial and temporal variability of saturated soil hydraulic conductivity at the field-scale. *Soil Tillage Res.* **2014**, *135*, 28–40. [[CrossRef](#)]
31. Kelishadi, H.; Mosaddeghi, M.; Hajabbasi, M.; Ayoubi, S. Near-saturated soil hydraulic properties as influenced by land use management systems in Koohrang region of central Zagros, Iran. *Geoderma* **2014**, *213*, 426–434. [[CrossRef](#)]
32. Reichert, J.M.; Suzuki, L.E.A.S.; Reinert, D.J.; Horn, R.; Håkansson, I. Reference bulk density and critical degree-of-compactness for no-till crop production in subtropical highly weathered soils. *Soil Tillage Res.* **2009**, *102*, 242–254. [[CrossRef](#)]
33. Kaufmann, M.; Tobias, S.; Schulin, R. Comparison of critical limits for crop plant growth based on different indicators for the state of soil compaction. *J. Plant Nutr. Soil Sci.* **2010**, *173*, 573–583. [[CrossRef](#)]
34. Šimůnek, J.; van Genuchten, M.T.; Šejna, M. Development and applications of the HYDRUS and STANMOD software packages and related codes. *Vadose Zone J.* **2008**, *7*, 587–600. [[CrossRef](#)]
35. Van Genuchten, M.T. A closed-form equation for predicting the hydraulic conductivity of unsaturated soils. *Soil Sci. Soc. Am. J.* **1980**, *44*, 892–898. [[CrossRef](#)]
36. Schaap, M.G.; Leij, F.J.; Van Genuchten, M.T. Rosetta: A computer program for estimating soil hydraulic parameters with hierarchical pedotransfer functions. *J. Hydrol.* **2001**, *251*, 163–176. [[CrossRef](#)]
37. Bormann, H.; Klaassen, K. Seasonal and land use dependent variability of soil hydraulic and soil hydrological properties of two Northern German soils. *Geoderma* **2008**, *145*, 295–302. [[CrossRef](#)]
38. Alletto, L.; Coquet, Y. Temporal and spatial variability of soil bulk density and near-saturated hydraulic conductivity under two contrasted tillage management systems. *Geoderma* **2009**, *152*, 85–94. [[CrossRef](#)]

39. Chirico, G.B.; Medina, H.; Romano, N. Uncertainty in predicting soil hydraulic properties at the hillslope scale with indirect methods. *J. Hydrol.* **2007**, *334*, 405–422. [[CrossRef](#)]
40. Poudel, D.D.; Ferris, H.; Klonsky, K.; Horwath, W.R.; Scow, K.M.; van Bruggen, A.H.; Lanini, W.T.; Mitchell, J.P.; Temple, S.R. The sustainable agriculture farming system project in California's Sacramento Valley. *Outlook Agric.* **2001**, *30*, 109–116. [[CrossRef](#)]
41. Schnug, E.; Rogasik, J.; Panten, K.; Paulsen, H.M.; Haneklaus, S. Ökologischer Landbau erhöht die Versickerungsleistung von Böden—ein unverzichtbarer Beitrag zum vorbeugenden Hochwasserschutz. *Okol. Landbau* **2004**, *32*, 53–55.
42. Schnug, E.; Haneklaus, S. Agricultural production techniques and infiltration significance of organic farming for preventive flood protection. *Landbauforsch. Völkenrode* **2002**, *52*, 197–203.
43. Delleur, J.W. Soil Properties and Moisture Movement in the Unsaturated Zone. In *The Handbook of Groundwater Engineering*; CRC Press: Boca Raton, FL, USA, 2006; pp. 255–314.
44. Vereecken, H.; Kasteel, R.; Vanderborght, J.; Harter, T. Upscaling Hydraulic Properties and Soil Water Flow Processes in Heterogeneous Soils: A Review. *Vadose Zone J.* **2007**, *6*, 1–28. [[CrossRef](#)]
45. Abu-Hashim, M.; Mohamed, E.; Belal, A.-E. Identification of potential soil water retention using hydric numerical model at arid regions by land-use changes. *Int. Soil Water Conserv. Res.* **2015**, *3*, 305–315. [[CrossRef](#)]
46. Abd-Elmabod, S.K.; Mansour, H.; Hussein, A.; Jordán, A. Influence of irrigation water quantity on the land capability classification. *Plant Arch* **2019**, *2*, 2253–2561.
47. Jacques, D.; Mohanty, B.P.; Feyen, J. Comparison of alternative methods for deriving hydraulic properties and scaling factors from single-disc tension infiltrometer measurements. *Water Resour. Res.* **2002**, *38*, 25-1–25-14. [[CrossRef](#)]
48. Droogers, P.; Bouma, J. Biodynamic vs. conventional farming effects on soil structure expressed by simulated potential productivity. *Soil Sci. Soc. Am. J.* **1996**, *60*, 1552–1558. [[CrossRef](#)]
49. Oquist, K.; Strock, J.S.; Mulla, D. Influence of alternative and conventional management practices on soil physical and hydraulic properties. *Vadose Zone J.* **2006**, *5*, 356–364. [[CrossRef](#)]
50. Said, M.E.S.; Ali, A.M.; Borin, M.; Abd-Elmabod, S.K.; Aldosari, A.A.; Khalil, M.M.; Abdel-Fattah, M.K. On the use of multivariate analysis and land evaluation for potential agricultural development of the northwestern coast of Egypt. *Agronomy* **2020**, *10*, 1318. [[CrossRef](#)]
51. Mohamed, E.; Abdellatif, M.; Abd-Elmabod, S.K.; Khalil, M. Estimation of surface runoff using NRCS curve number in some areas in northwest coast, Egypt. In *E3S Web of Conferences*; EDP Sciences: Les Ulis, France, 2020; p. 02002.
52. El Nahry, A.H.; Mohamed, E.S. Potentiality of land and water resources in African Sahara: A case study of south Egypt. *Environ. Earth Sci.* **2011**, *63*, 1263–1275. [[CrossRef](#)]
53. Mohamed, E.S.; Baroudy, A.A.; El-beshbeshy, T.; Emam, M.; Belal, A.A.; Elfadaly, A.; Aldosari, A.A.; Ali, A.M.; Lasaponara, R. Vis-nir spectroscopy and satellite landsat-8 oli data to map soil nutrients in arid conditions: A case study of the northwest coast of Egypt. *Remote Sens.* **2020**, *12*, 3716. [[CrossRef](#)]